Exploring phase control in a quantum dot light-emitting diode

H Al Husseini[1], SF Abdalah[2], KAM Al Naimee[2,3] $\textcolor{green}{\circledR}$, R Meucci[2],
and FT Arecchi[2,4]

Abstract

We report phase control in a periodically driven chaotic nanosystem consisting of a quantum dot light-emitting diode. Such a dynamical system is a class C laser, whence the charactering features are intrinsically chaotic. Phase control relies on the addition of small parametric harmonic perturbations with adjustable phase. Phase control is demonstrated by changing both frequency and strength of the controlling perturbations. Our results show that phase control has two crucial effects on a quantum dot light-emitting diode. First, it can enhance the spiking behavior in either regular or chaotic regimes; second, it is able to turn periodic behavior to chaotic behavior with a minimal perturbation when a resonance condition at half of the driving frequency is achieved.

Introduction

Chaos control methods are usually classified within two main categories depending on how they interact with the chaotic system, that is, feedback and nonfeedback methods.[1,2] In feedback methods, small state-dependent perturbations are applied to the chaotic system.[3,4] While in nonfeedback methods, small harmonic perturbations are added.[5,6] Among the nonfeedback techniques, phase control of chaos plays a crucial role. In this control, the key parameter is the phase difference between the main driving responsible for the appearance of chaos (we are considering nonautonomous dynamical systems) and an external harmonic perturbation. The phase control strategy in chaos has been demonstrated in different systems.[5–15]

In this article, we study the phase control of a current modulated quantum dot light-emitting diode (QD-LED). QD-LEDs and organic LEDs (OLEDs) are alternative technologies to the consolidated one of solid-state LEDs.[16] The interest in QD-LEDs, first reported by Colvin et al.,[17] is growing up dramatically considering the better luminescent properties compared with those of OLEDs.[18,19] For these reasons, QD-LEDs represent promising devices in optoelectronic applications for high-quality fast-moving images, short-distance optical fiber communications, and lightweight and low-power consumption. Apart from technological applications, QD-LEDs are interesting for their dynamical properties. The QD-LED dynamics can be modeled by three equations for three populations, namely, photon number in the optical mode, population of carriers in the QD well, and population of carriers in the wetting layer (WL).[20,21] In this model, chaos can emerge in a spontaneous way; in other terms, according to the classification introduced by Arecchi et al.,[22] a QD-LED is equivalent to a class C laser, such as FIR lasers where photon number, population inversion between the two lasing levels, and polarization are characterized by the same time scales and chaos can be reached by adjusting the control parameters.

[1] Nassiriya Nanotechnology Research Laboratory, College of Science, Thi-Qar University, Nassiriyah, Iraq
[2] Istituto Nazionale di Ottica-CNR, Firenze, Italy
[3] Department of Physics, College of Science, University of Baghdad, Baghdad, Iraq
[4] Università degli Studi di Firenze, Firenze, Italy

Corresponding author:
KAM Al Naimee, Istituto Nazionale di Ottica-CNR, Firenze, Italy; Department of Physics, College of Science, University of Baghdad, Baghdad, Iraq.
Email: kais.al-naimee@ino.it

Class B lasers are instead described by only two variables, namely, photon numbers and population inversion. As a consequence, the appearance of chaos in class B requires the introduction of external modulations or additional feedbacks such as optoelectronic or optical as it commonly occurs in semiconductor lasers. This issue had been addressed in QD lasers when they have been treated as class B lasers.[23,24]

A QD-LED can be perturbed by applying an external sinusoidal modulation of the injection current, which is the only accessible control parameter. The emerging chaos has different properties from those ones emerging spontaneously by steadily adjusting the injection current.

The phase control of chaos that is considered here requires an external modulation frequency, playing the role of an intrinsic reference clock for a control frequency with adjustable phase shift. This is the key ingredient of such a control strategy. In this article, the frequency ratio between these two frequencies will be varied, showing interesting phenomena that make this strategy important for chaotic encryption. It is important to note that this control strategy is not apt to stabilize fixed-point or steady-state solutions. In such cases, feedback methods based on the derivative of the laser output intensity have been successfully tested on class B lasers.[25,26] We also note that phase control can be applied in a pulsed way. However, the role of the harmonic content of a periodic pulsed perturbation has nontrivial effects as recently demonstrated in a driven Duffing oscillator.[27]

The article is organized as follows. In "The rate equation model and phase control" section, we describe the dynamical system and its phase control. In the "Controlled bifurcation scenarios" section, the effects of different external modulation frequencies and modulation depths are presented. Concluding remarks and notes are reported in the "Concluding remarks" section.

The rate equation model and phase control

The model is shown in Figure 1. It considers a nanostructure where electrons are first injected into the WL, before they are captured by the QDs. The underlying dynamics is described by the following nonlinear rate equations for the number of carriers in the QD ground state, n_{QD}; the number of carriers in the WL, n_{wl}; and the number of photons in the optical mode, S

$$\dot{S} = Wn_{QD}^2 - Wn_{QD}S - \gamma_s S \tag{1}$$

$$\dot{n}_{QD} = \gamma_C n_{wl}\left(1 - \frac{n_{QD}}{2N_d}\right) - \gamma_{r_{QD}}n_{QD} - (Wn_{QD}^2 - Wn_{QD}S) \tag{2}$$

$$\dot{n}_{wl} = \frac{I(t)}{e} - \gamma_{r_{wl}}n_{wl} - \gamma_C n_{wl}\left(1 - \frac{n_{QD}}{2N_d}\right) \tag{3}$$
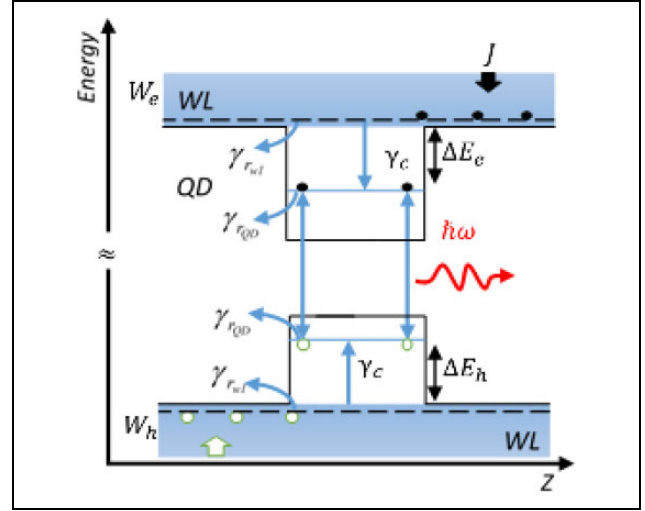
Figure 1. Energy diagram illustrating the recombination mechanisms in active layer QD-LED. QD-LED: quantum dot light-emitting diode.

The processes of spontaneous emission and reabsorption in QDs are modeled by the first and second terms of equation (1), where W is the Einstein coefficient given by $W = [(|\mu|^2 \sqrt{\varepsilon_{bg}})/(3\pi\varepsilon_o\hbar)]/(w/c)^3$. ε_{bg} is the static relative permittivity of the background medium, ε_o is the vacuum permittivity, c is the speed of light in vacuum, μ is the dipole moment, $\hbar$ is Planck's constant, and ω is the frequency. $\gamma_{r_{QD}}$ and $\gamma_{r_{wl}}$ are the non-radiative decay rates of the number of carriers in the QD and WL, respectively; N_d is the total number of QDs. e is electron charge, γ_c is the capture rate from WL into the dot, and γ_s is the output coupling rate of photons in the optical mode. The time-dependent injection current $I(t)$ is given by $I(t) = I_{dc} + I_{ac}\sin(2\pi f_m t)$, where I_{dc} and I_{ac} are the *dc* and *ac* part of the injection current, respectively, and f_m is the modulation frequency.

The model is simplified by introducing dimensionless variables and parameters, namely

$$x = S, \quad y = \frac{W}{\gamma_s}n_{QD}, \quad z = \frac{n_{wl}\gamma_c}{W}, \quad \gamma = \frac{\gamma_s}{\gamma_{r_{wl}}}, \quad \gamma_1 = \frac{W}{\gamma_s},$$

$$\gamma_2 = \frac{W}{\gamma_{r_{wl}}}, \quad \gamma_3 = \frac{\gamma_{r_{QD}}}{\gamma_{r_{wl}}}, \quad \gamma_4 = \frac{\gamma_c}{\gamma_{r_{wl}}}, \quad N_d \equiv a,$$
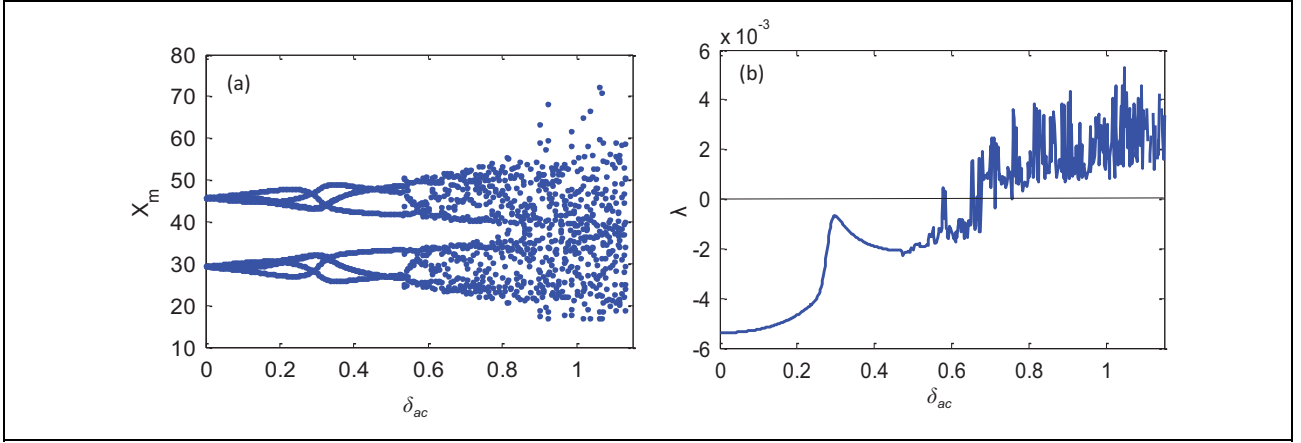
$$\delta_o(t') = \frac{I(t)}{We}, \quad f'_m = f_m/\gamma_{r_{wl}}, \quad \text{and } t' = \gamma_{r_{wl}}t$$

The dimensionless dynamical system assumes the form

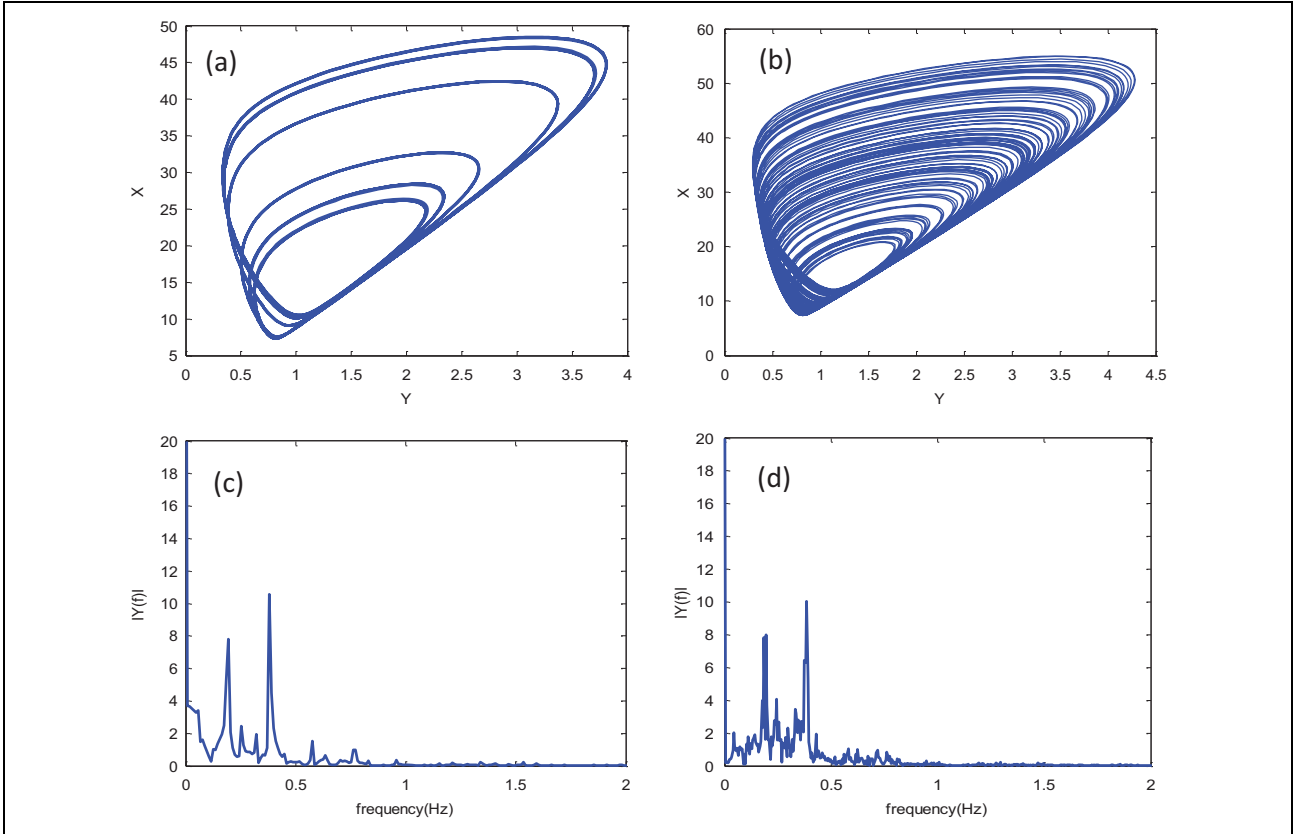$$\gamma_1\dot{x} = \gamma\left(y^2 - \gamma_1 x(y+1)\right) \tag{4}$$

$$\dot{y} = \gamma_2 z\left(\gamma_1 - \frac{y}{2a}\right) - y(\gamma_3 + \gamma y) + \gamma_2 xy \tag{5}$$

$$\dot{z} = \gamma_4\left(\delta_o(t') - z + \frac{yz}{2\gamma_1 a}\right) - z \tag{6}$$

Figure 2. (a) Bifurcation diagram of the photon density versus modulation depth δ_{ac}; $\delta_{dc} = 0.15$, $f'_m = 8 \times 10^{-2}$ ($t' = 1 \times 10^3$). (b) Maximal Lyapunov exponent versus δ_{ac}.

Figure 3. x–y representation of the attractors at (a) $\delta_{ac} = 0.4$ and (b) $\delta_{ac} = 1$ for a value of $\delta_{dc} = 0.15$ and $f'_m = 8 \times 10^{-2}$. (c) and (d) Power spectra of (a) and (b), respectively.

Here, the upper subscript "dot" refers to differentiation with respect to t'. The bias current is now represented by

$$\delta_o(t') = \delta_{dc} + \delta_{ac} \sin(2\pi f'_m t') \qquad (7)$$

We characterize the system dynamics, by its bifurcation diagram and Lyapunov exponent (LE). The bifurcation diagram yields the asymptotic behavior of the system. The LE shows how the close trajectories are separated.

In Figure 2(a), the bifurcation diagram of the x variable (photon number) as a function of δ_{ac} at fixed value of modulating frequency $f'_m = 8 \times 10^{-2}$ is reported. The system evolves from a period-2 solution to chaos after bifurcations involving period-3 solutions (a stable period-6 solution is present at $\delta_{ac} = 0.4$). Figure 2(b) shows the corresponding maximal LE which gets positive as the modulation depth is nearly equal to seven. In Figure 3(a) and

(b), we report an *x–y* representation of a stable period-6 solution and of chaotic attractor at a modulation depth δ_{ac} = 0.4 and δ_{ac} = 1, respectively. In Figure 3(c) and (d), the corresponding Fourier spectra are presented. The power spectra show distinctive subharmonic peaks in particular at first subharmonic of the fundamental modulating
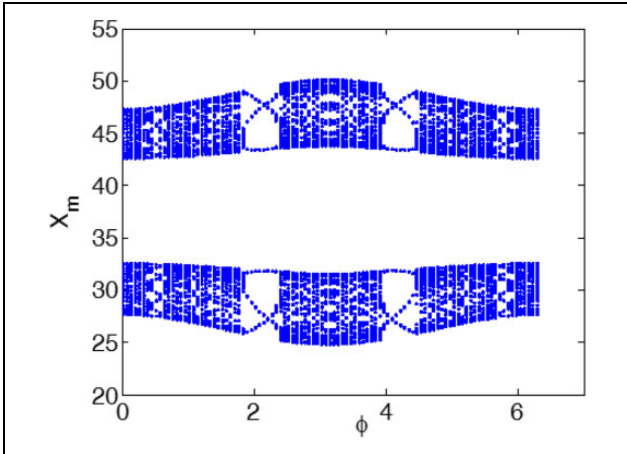
Figure 4. Bifurcation diagram of the photon density versus modulation phase φ. Frequency ratio $m = 1$, $\varepsilon = 0.1$.

frequency which will influence the dynamics when phase control technique is introduced. As already stated above, this nonfeedback technique exploits the role of additional sinusoidal perturbations to the main forcing frequency at $f'_m = 8 \times 10^{-2}$. As reference condition on which phase control will be applied, we consider the periodic dynamics at $\delta_{ac} = 0.3$ (see Figure 2(a)).

In the presence of phase control, the bias current $\delta_o(t')$ in equation (7) is replaced by

$$\delta'_o(t') = \delta_{dc} + \delta_{ac}\left(1 + \varepsilon \sin\left(2\pi m\, f'_m t' + \varnothing\right)\right) sin\left(2\pi f'_m t'\right)$$

(8)

where *m* is the frequency ratio in which our investigations will assume integer and fractional values. Once *m* is fixed, the two parameters for our control are the perturbation strength ε and phase difference φ.

Controlled bifurcation scenarios

Let us first consider the effects of the phase difference φ on the dynamics at the resonant case $m = 1$, that is, when the added perturbing frequency is equal to the main modulation frequency. The controlled dynamics is presented in Figure 4
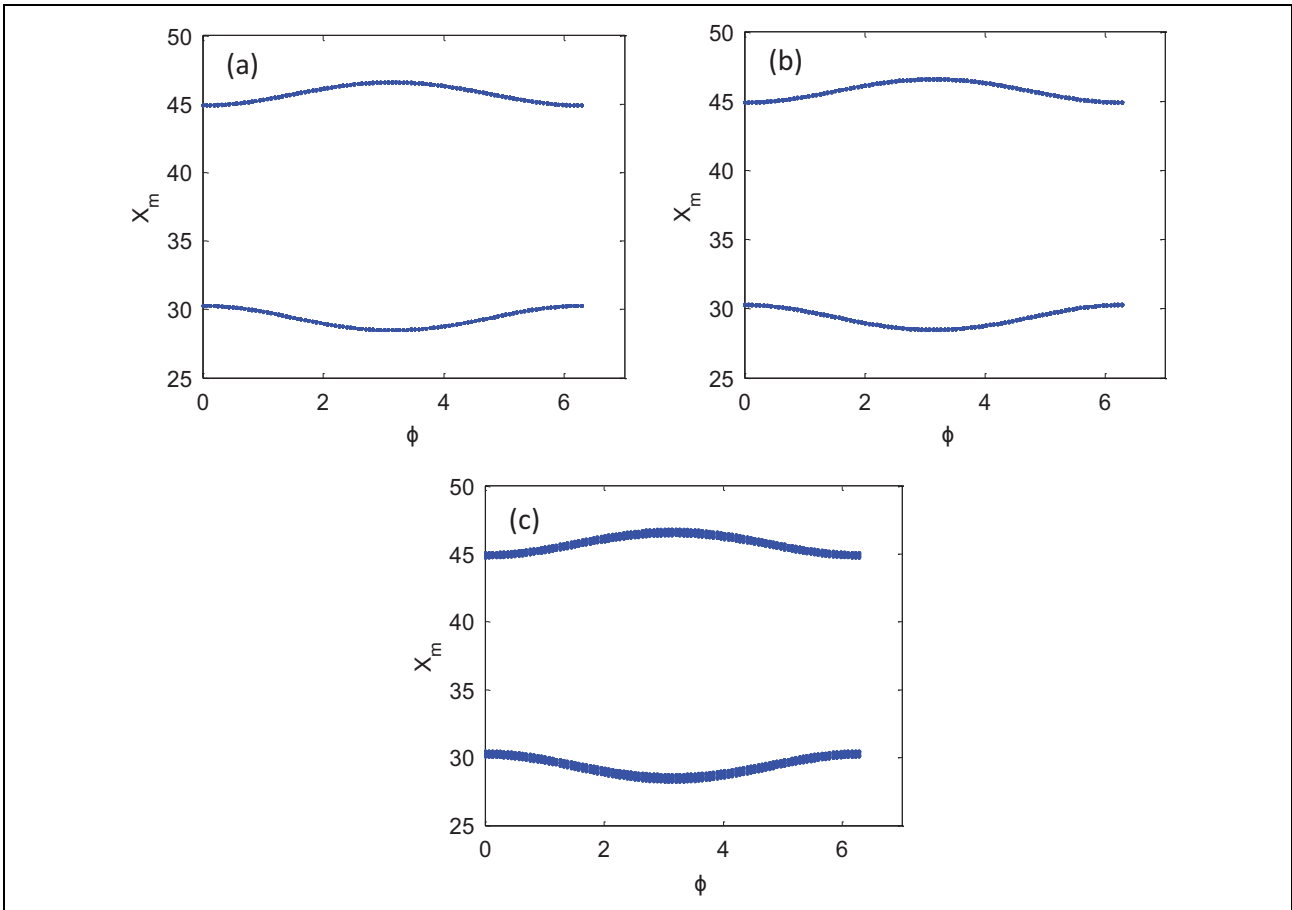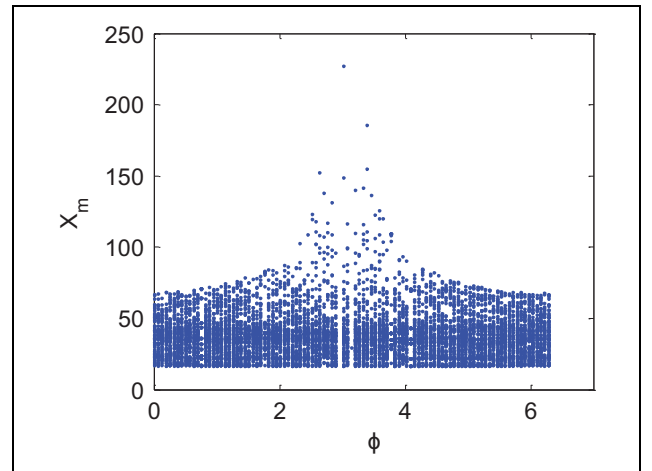

Figure 5. Bifurcation diagram of the photon density versus modulation phase φ for (a) $m = 4$, (b) $m = 3$, and (c) $m = 2$. $\varepsilon = 0.1$.
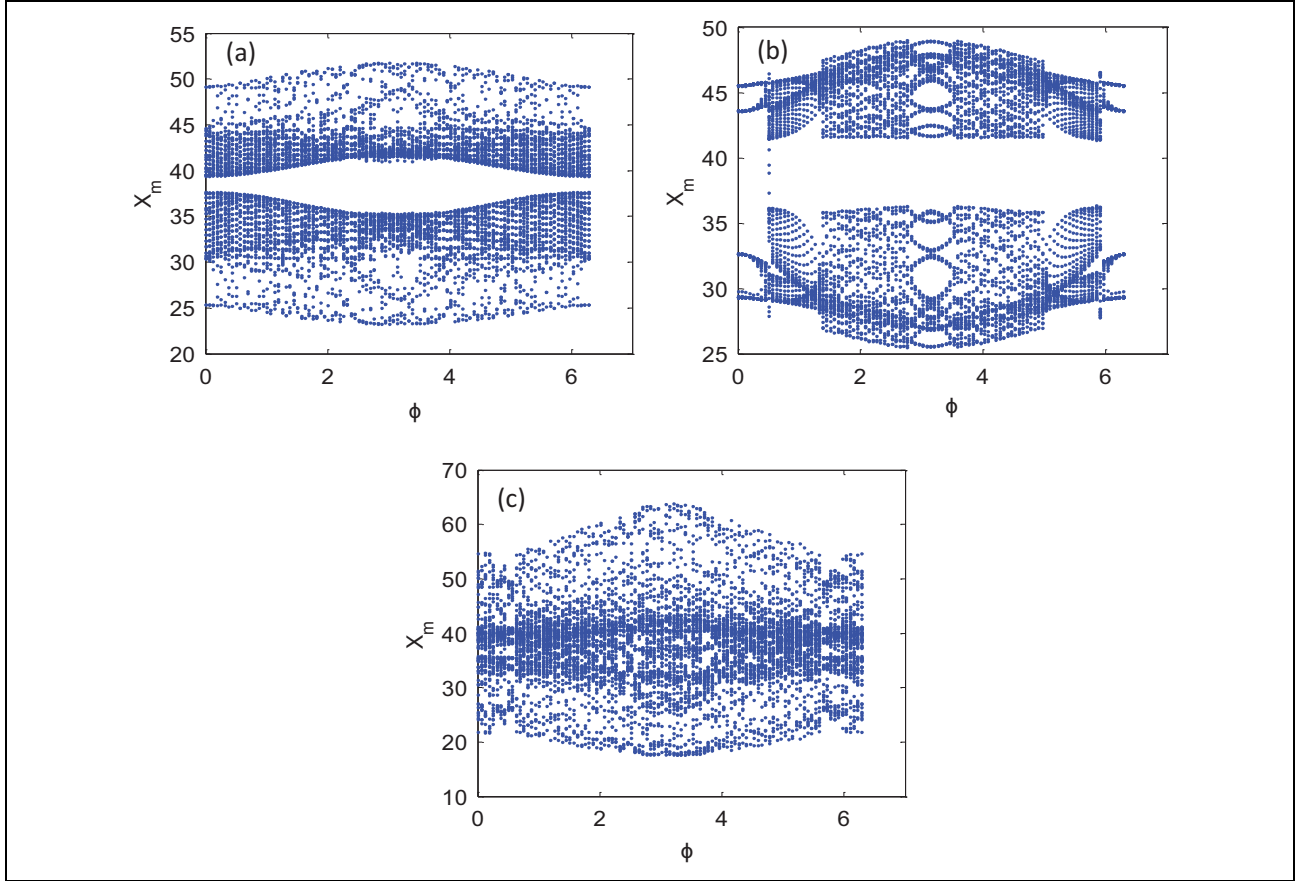
Figure 6. Bifurcation diagram of the photon density versus modulation phase φ for (a) $m = 0.9$, (b) $m = 0.8$, and (c) $m = 0.6$. $\varepsilon = 0.1$.

as the phase φ is increased from 0 to 2π (the perturbation strength is kept fixed at $\varepsilon = 0.1$). The effects of phase control are remarkable. An unperturbed periodic behavior is changed in chaotic one except two periodic windows around $\varphi = \pi$. These two distinct and symmetric regions are clearly detectable in Figure 4. When the frequency ratio m is higher than 1 (2, 3, and 4), the bifurcation diagrams show only periodic solutions of period 2 (see Figure 5). This indicates that the QD-LED dynamics is stabilized to the unperturbed period-2 solution in the bifurcation diagram (Figure 2(a)) at $\delta_{ac} = 0$. The controlled bifurcation diagrams become broadened (roof and floor) and show a weak dependency on φ.

Different scenarios occur when the frequency ratio m assumes values less than 1. The controlled bifurcation diagrams for $m = 0.9$ (Figure 6(a)) and $m = 0.8$ (Figure 6(b)) show two separated chaotic bands around the stabilized solutions of period 2. The band separation disappears at $m = 0.6$, as shown in Figure 6(c). The merging of the two chaotic bands means that the frequency ratio m is approaching the golden mean ratio $1/1.6180 = 0.61$ and as a consequence we are in the presence of quasiperiodic chaos.[28] In other terms, the perturbing frequency competes with the driving frequency inducing torus breaking. A similar phenomenon has been reported in modulated external-cavity

Figure 7. Bifurcation diagram of the photon density versus modulation phase φ at $m = 0.5$ and $\varepsilon = 0.1$.

semiconductor lasers by Lam et al.[29,30] In these articles, however, the key role of the relative phase between the two competing frequencies has not been addressed.

A pathological condition is reached at the frequency ratio $m = 0.5$ (see Figure 7). In such condition, the system shows a resonance at $\varphi = \pi$. The chaotic attractor has amplitudes about one order of magnitude larger than the
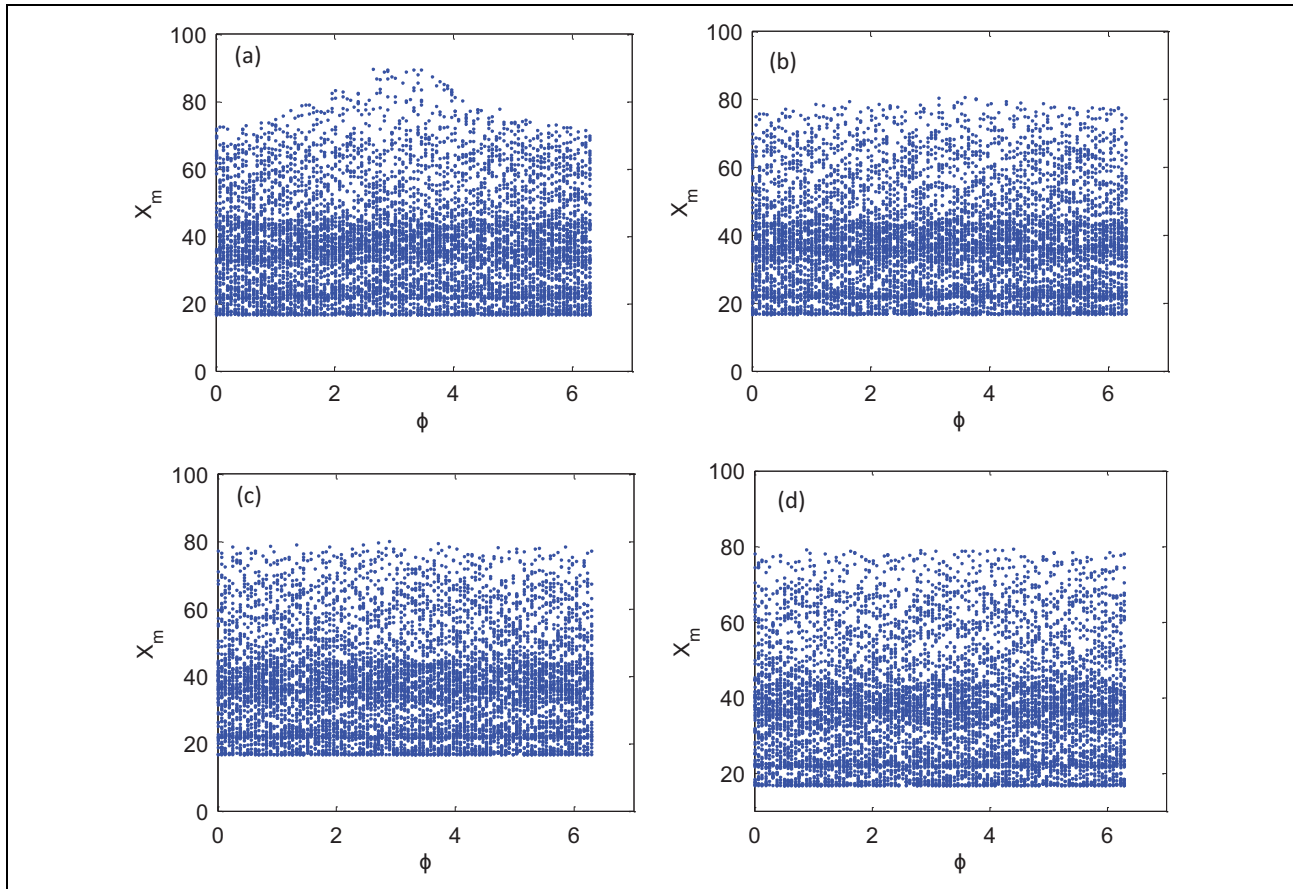
Figure 8. Bifurcation diagram of the photon density versus modulation phase φ for (a) $\varepsilon = 0.05$, (b) $\varepsilon = 0.01$, (c) $\varepsilon = 0.005$, and (d) $\varepsilon = 0.001$. $m = 0.5$.

unperturbed condition at $\delta_{ac} = 0.3$. The chaotic amplitude at the resonance condition at $m = 0.5$ and $\varphi = \pi$ can be mitigated by decreasing the perturbation strength ε. As the parameter ε is decreased by more than two order of magnitude ($\varepsilon = 0.005$), the phase effect at $\varphi = \pi$ is reduced up to its complete disappearance, as shown in Figure 8. Also the chaotic attractor maximal amplitude is stabilized. This means that the system displays its maximal sensitivity to its first subharmonic resonance component ($m = 0.5$). In this condition, a relative perturbation of 5% modulation depth is sufficient to change chaotic attractors sensitive to phase difference φ to chaotic attractors insensitive to the phase.

Concluding remarks

In this work, phase control has been applied to the chaotic dynamics in a QD-LED. We have demonstrated that phase control has crucial effects on the unperturbed dynamics. First, it can enhance the behavior in either regular or chaotic regime when the frequency ratio m is varied. These features can be used in telecommunication-based applications, where a chaotic carrier is commonly used to convey information in a secure channel. Phase control could be employed to select and tune a particular dynamic regime

sensitive or insensitive to the phase differences between a modulating carrier frequency and a second perturbing frequency.

Declaration of conflicting interests

The author(s) declared no potential conflicts of interest with respect to the research, authorship, and/or publication of this article.

ORCID iD

KAM Al Naimee 🄳 http://orcid.org/0000-0002-7682-4829

References

1. Scholl E and Schuster HE (ed). *Handbook of chaos control*. Berlin: Wiley-VCH, 2007.
2. Boccaletti S, Grebogi C Lai YC, et al. The control of chaos: theory and applications. *Phys Rep* 2000; 329: 103.

3. Ott E, Grebogi C and Yorke JA. Controlling chaos. *Phys Rev Lett* 1990; 64: 1196.

4. Pyragas K. Continuous control of chaos by self-controlling feedback. *Phys Lett A* 1992; 170: 491.

5. Meucci R, Gadomski W, Ciofini M, et al. Experimental control of chaos by means of weak parametric perturbations. *Phys Rev E Stat Phys Plasmas Fluids Relat Interdiscip Topics* 1994; 49: R2528–R2531.

6. Meucci R, Euzzor S, Pugliese E, et al. Optimal phase-control strategy for damped-driven Duffing oscillators. *Phys Rev Lett* 2016; 116: 044101.

7. Qu Z, Hu G, Yang G, et al. Phase effect in taming nonautonomous chaos by weak harmonic perturbations. *Phys Rev Lett* 1995; 74: 1736.

8. Yang J, Qu Z and Hu G. Duffing equation with two periodic forcings: the phase effect. *Phys Rev E* 1996; 53: 4402.

9. Chacon R. Suppression of chaos by selective parametric perturbations. *Phys Rev E Stat Phys Plasmas Fluids Relat Interdiscip Topics* 1995; 51: 761–764.

10. Chacon R. Role of ultra-subharmonic resonances in taming chaos. *Europhys Lett* 2001; 54: 148.

11. Cao H, Chi X and Chen G. Suppressing or inducing chaos by weak resonant excitations. *Int J Bifurcation Chaos Appl Sci Eng* 2004; 14: 1115.

12. Leung AYT and Zengrong L. Suppressing chaos for some nonlinear oscillators. *Int J Bifurcation Chaos Appl Sci Eng* 2004; 14: 1455.

13. Seoane JM, Zambrano S, Euzzor S, et al. Avoiding escapes in open dynamical systems using phase control. *Phys Rev E Stat Nonlin Soft Matter Phys* 2008; 78: 016205.

14. Chacon R, MartínezGarcía-Hoz A, Miralles JJ, et al. Amplitude modulation control of escape from a potential well. *Phys. Lett A* 2014; 378: 1104.

15. Zambrano S, Seoane JM, Mariño IP, et al. Phase control of excitable systems. *New Journal of Physics* 2008; 10: 073030.

16. Reineke S. Complementary LED technologies. *Nat Mater* 2015; 14: 459–462.

17. Colvin VL, Schlamp MC and Alivisatos AP. Light-emitting diodes made from cadmium selenide nanocrystals and a semiconducting polymer. *Nature* 1994; 370: 354–357.

18. Kim KH, Lee S, Moon CK, et al. Phosphorescent dye-based supramolecules for high-efficiency organic light-emitting diodes. *Nat Commun* 2014; 5: 4769.

19. Liu S, Liu W, Ji W, et al. Top-emitting quantum dots light-emitting devices employing microcontact printing with electricfield-independent emission. *Sci Rep* 2016; 6: 22530.

20. Al Naimee K, Al Husseini H, Abdalah SF, et al. Complex dynamics in quantum dot light emitting diodes. *Eur Phys J D* 2015; 69: 257.

21. Al Husseini HB., Al Naimee KA, Khidhir Ali H, et al. Dynamics of quantum dot light-emitting diode with filtered optical feedback. *Nanomaterials and Nanotechnology*, 2016; 6: 1–9.

22. Arecchi FT, Lippi GL, Puccioni GP, et al. Deterministic chaos in lasers with injected signal. *Opt Comm* 1984; 51: 308.

23. Erneux T, Viktorov EA, Kelleher B, et al. Optically injected quantum-dot lasers. *Opt Lett*. 2010; 35: 937–939.

24. Ludge K, Bormann MJP, Malić E, et al. Turn-on dynamics and modulation response in semiconductor quantum dot lasers. *Phys Rev B* 2008; 78: 035316.

25. Bielawski S, Bouazaoui M, Derozier D, et al. Stabilization and characterization of unstable steady states in a laser. *Phys Rev A* 1993; 47: 3276.

26. Ciofini M, Labate A, Meucci R, et al. Stabilization of unstable fixed points in the dynamics of a laser with feedback. *Phys Rev E* 1999; 60: 398–402.

27. Arecchi FT, Euzzor S, Gallas MR, et al. Exploring phase control with square pulsed perturbations. *Eur Phys J Special Topics* 2017; 226: 1785–1790.

28. Ott E. *Chaos in dynamical systems*. Cambridge: Cambridge University Press, 1993.

29. Lam BC, Kellner AL, Sushchik MM, et al. Observation of chaotic instability in the active mode locking of a semiconductor laser. *J Opt Soc Am B* 1993; 10: 2065–2070.

30. Lam BC, Sushchik MM, Abarbanel HDI, et al. Relaxation-oscillation-induced chaotic instabilities in modulated external-cavity semiconductor lasers. *J Opt Soc Am B* 1995; 12: 1150–1156.